NUCLEAR REACTIONS
(THEORETICAL)

CASCADE CALCULATIONS FOR NUCLEUS-NUCLEUS COLLISIONS

G. Bertsch, S. Das Gupta, H. Kruse, B. Jacak and H. Stöcker

A recent article by Stock, et al.,[1] suggests that the nuclear equation of state might be measured by the pion production cross section in heavy ion collisions. In this note we point out that the pion production cross sections, as determined by cascade model calculations, do not permit firm conclusions about the nuclear equation of state, since too many unknown aspects of nucleon physics have been left out in the model calculation used. In order to conclude whether pion cross sections are sensitive to the equation of state, the cascade must be improved by at least including potential field effects and the Pauli principle. We have modified a simple cascade program to take these effects into account. The theory is based on the Boltzmann equation,

$$\frac{\partial f}{\partial t} + v\cdot\nabla_r f - \nabla U\cdot\nabla_p f = -\int \frac{d^3p_2 d^3p_1' d^3p_2'}{(2\pi)^9} v_{12}\sigma$$

$$[f_2(1-f_{1'})(1-f_{2'}) - f_{1'}f_{2'}(1-f_2)(1-f)]$$

$$(2\pi)^3\delta^3(p+p_2-p_1'-p_2')$$

Here f(p,r) is the phase space distribution function, represented by the density of particles in the cascade, and U(f) is a mean potential field. The Pauli principle enters the theory only via the initialization of the distribution function and the (1-f) factors in the Uehling-Uhlenbeck collision integrals.[2]

In the framework of the usual cascade model, it is not possible to determine f and U accurately enough to be useful. We circumvent this by using an ensemble of cascade runs to determine f as a function of time. Specifically, our algorithm for f is

$$f_{num}(p,r) = \sum_i^N \frac{n_i}{N\Omega(p,r)} \qquad (1)$$

where $\Omega(p,r)$ is a volume of phase space centered at (p,r), n_i is the number of particles in that volume at a given time in a specific cascade run, and N is the number of runs in the ensemble. Collisions in the cascade runs are treated in the usual way, except that collisions are stochastically Pauli blocked using a blocking probability

$$P_{block} = 1-(1-f_{num}(1'))(1-f_{num}(2')) \quad \text{if } f_{num}(1') \text{ and } f_{num}(2')<1.$$

$$= 1 \text{ if either } f_{num}(1')\geq 1 \text{ or } f_{num}(2')\geq 1. \qquad (2)$$

Some feeling for the accuracy of this procedure can be obtained by studying the systematic error, which arises because Eq. (2) is only unbiased if f_{num} never exceeds 1. Defining $\bar{f}_{num}=\min(f_{num}, 1)$, we find that average $\bar{f}_{num}$ values of 0.80 can be obtained rather easily when f=1 for the actual distribution function. Our preliminary results are that the Pauli principle makes negligible difference in the pion production for bombarding energies in the range 400-800 MeV/n.

The mean field is calculated as a uniform potential in coordinate space cubes of side 2 fm, and the value of the potential is determined from the density of particles,

$$\rho_{num} = \frac{\sum_k n_i}{N(2fm)^3}$$

The potential field can be chosen as a simple function of ρ_{num} by considering the simplified Skyrme interaction. We will consider two extremes. One is a stiff equation of state (K=375) with U given by the function

$$U = -124\ \rho/\rho_0 + 70.5(\rho/\rho_0)^2 \text{ MeV} \qquad (3)$$

where $\rho_0=0.16$ fm^{-3} is ordinary nuclear matter density. The other extreme is a soft equation of state (K=200), with U given by

$$U = -356\ \rho/\rho_0 + 303(\rho/\rho_0)^{7/6} \text{ MeV} \qquad (4)$$

We have preliminary results on the effect of the mean field on pion production. Both soft and stiff models of the mean field yield pion production rates close to those of the simple cascade. If these results stand, the conclusion will be that pion production cannot be used to infer the equation of state, contradicting Ref. 1.

In addition to the consideration outlined above, we have included in the cascade calculations a proper treatment of isospin effects, i.e. we distinguish between 2 nucleons, 4 delta particles and 3 pions. This modification has several advantages: (1) We can use experimental cross sections directly, without isospin averaging. In this context it is worthwhile to mention that the parametrizations commonly used in isospin-averaged calculations do not describe the p-p or p-n cross sections too well in the region where pion production has recently drawn so much attention (400-1800 MeV Lab energy). Even though the error in using isospin averaged cross sections may not be large, it is certainly desirable to use the exact experimental numbers as input when searching for exotic effects in heavy ion collisons. (2) The p-n, T=0 nonresonant pion production at higher energies can be included. (3) Asymmetric systems with projectiles and targets which differ widely in

their N/Z ratios can be treated properly. In particular this influences the ratio of production of charged to neutral pions.

1. R. Stock, et al., Phys. Rev. Lett. 49 (1982) 1236; J. Cugnon, et al., Nucl. Phys. A379 (1982) 553.
2. E.A. Uehling and G.E. Uhlenbeck, Phys. Rev. 43 (1933) 552.

SUBBARRIER FUSION

H. Esbensen, J.-Q. Wu and G.F. Bertsch

The fusion cross section of intermediate heavy nuclei is usually quite well described in terms of one-dimensional barrier penetration models, providing the energy is above the Coulomb barrier. Recent experiments, with fusion cross sections in the region of 1 μb to 1 mb, clearly exhibit an enhancement compared to the predictions of such models. Other degrees of freedom must be important for the fusion process at subarrier energies, and we have studied in detail the influence of collective surface vibrations. Thus we consider a two-dimensional barrier penetration problem, one dimension being the radial separation of two ions and the other is the amplitude of a surface mode in one of the ions. The two degrees of freedom are coupled through the Coulomb and nuclear interactions.

We solve the time-independent Schrodinger equation for this problem in a coupled channel representation, and check the results in two extreme limits, viz. for $\omega \to 0$ (frozen approximation) and for $\omega \to \infty$ (adiabatic limit), where $\hbar\omega$ is the one-phonon excitation energy of the surface mode.

For a fixed value of the zero-point motion amplitude of the surface mode, the largest enhancement of the fusion probability is obtained in the frozen approximation. In this limit the zero-point motion of the surface mode leads to a fluctuation in the height of the barrier for the radial motion. The figure shows some contours of the two-dimensional density $|\psi(r,s)|^2$, where r is the radial separation and s is the amplitude of the surface mode. Inside the barrier (shaded area) the maximum of the density in the s-direction is seen to be shifted towards a

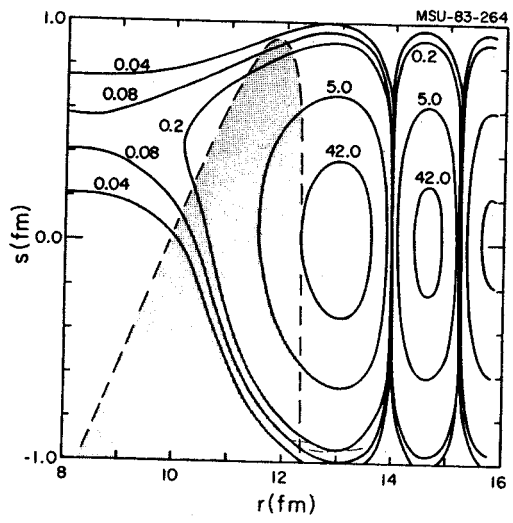

positive value of s, where the radial penetration probability is larger. The shift is proportional to the Coulomb force at the Coulomb barrier, so for heavy nuclei the fusion process probes the tail of the ground stat wave function of a surface mode.

For increasing values of $\hbar\omega$ the enhancement of the fusion probability decreases. This behavior is quite well reproduced by calculations based on an eikonal approximation in which the intrinsic motion of the surface mode is treated as a first order perturbation. In the adiabatic limit the barrier penetration reduces again to a one-dimensional problem.

In the reaction we have studied, ^{16}O + Sm, we find that the frozen approximation works quite well for the low-lying collective states in the Samarium isotopes. Giant resonances and states in ^{16}O contribute significantly to the enhancement of subbarrier fusion, but their contributions are reduced by adiabaticity.

NUCLEUS-NUCLEUS COLLISIONS IN THE CLASSICAL EQUATION-OF-MOTION MODEL

H. Kruse, J. Hoffer, and H. Stöcker

There have been several attempts to describe heavy ion collisions in the framework of classical, Newtonian equations of motion.[1] With the first experiments on the NSCL K500 cyclotron and the renewed interest in the medium (50-200 MeV/n) energy regime, it seems interesting to look again at the Newtonian approximation to the motion of the nucleons in the nucleus.

While this approach does not lend itself to the direct use of the experimental nucleon-nucleon scattering cross sections in the way a cascade approach does, it does have the advantage of treating the motion of each nucleon in the field of the remaining A-1 nucleons properly. It should therefore provide information about the heavy ion collisions which is complementary in many ways to the cascade approach.

We have chosen the nucleon-nucleon potential described in Ref. 1; the resulting classical scattering cross section is compared to the experimental differential cross section in Fig. 1. It should be mentioned that the scattering cross section is mainly governed by the strong repulsive hard core of the two-body potential; studies are currently underway to use the rms radius of the nucleus to determine the attractive portion of the potential.

The actual computer codes produced to solve the Newtonian equations of motion have the following properties:

(1) The equations were solved using both a second order leap-frog algorithm as well as a fifth order predictor-corrector. The former provides stable, fast solutions of the equations, while the latter allows the determination of extremely accurate solutions. When comparing individual trajectories, one finds that a very high (time-consuming) accuracy is required to provide reproducible solutions. However, most quantities of interest are statistical averages over many collisions, and we find that much less accuracy is required to compute these properly.

(2) A table lookup is used to avoid lengthy force calculations, and the lookup table is indexed using the square of the separation distance to avoid numerous square-root calculations.

(3) The leap-frog based code is capable of solving several collisions simultaneously to allow the computation of ensemble averages as a function of time.

Figure 2 shows the time sequence for a typical collision. We see that after the approach and interaction phases several nucleons and small clusters are emitted, leaving a heavy, excited fragment. The influence of the two-body scattering potential on the cluster formation, and the comparison of inclusive and exclusive cross sections with experimental data are currently under investigation.

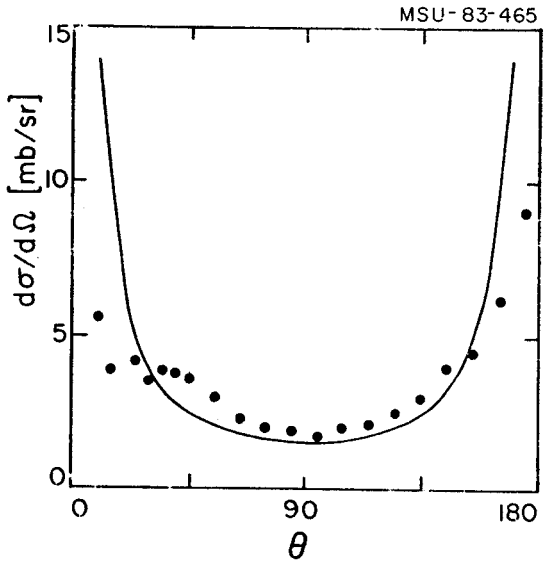

Fig. 1. The classical scattering cross section for two nucleons using the two-body potential of Ref. 1 is compared to the experimental differential cross section.

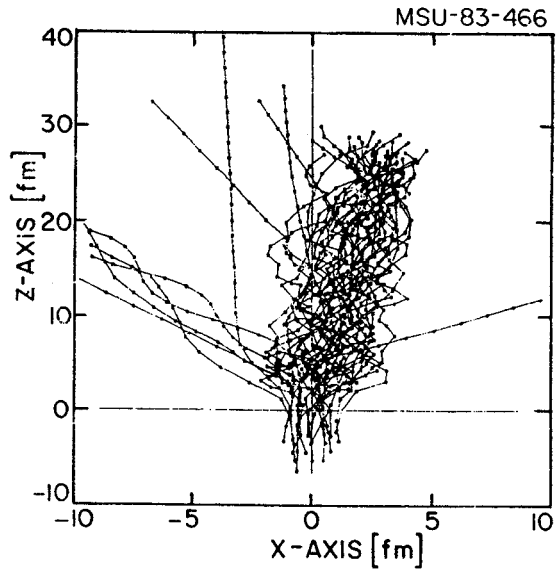

Fig. 2. Time sequence for the collision of two A=20 nuclei in the lab frame. The projectile travels along the z-axis from bottom to top. Each circle represents the position of a particle at equally spaced times. Subsequent positions of the same particle are connected by solid lines.

1. A.R. Bodmer et al., Phys. Rev. C15, 1342 (1977).

CALCULATION OF THE NUCLEAR-QUARK MATTER PHASE TRANSITION CURVE

C. Sanchez and H. Stöcker

We report on calculations of the temperature and density required to observe the postulated nuclear matter-quark gluon plasma transtion. The nuclear and quark matter are considered as two phases and it is required that the free energies of both phases be the same at the transition point. Since the density of quarks is three times the density of the baryons a transition curve can be calculated by solving:

$$\mu_b(P,T) = 3\mu_q(P,T)$$

where μ_b, μ_q refers to the chemical potential of the baryons and the quarks respectively. Alternatively, one may plot the pressure of both phases versus the baryon chemical potential for fixed temperature and determine the crossing point of both pressure curves.

The quark thermodynamical potential $\Omega=-P$ can be calculated in the framework of perturbative qcd in terms of an expansion in α, the strong (running) coupling constant of qcd,

$$\alpha = \frac{4\pi}{11-\frac{2}{3}N_f}\,\frac{1}{\ell n(m^2/\Lambda^2)}$$

where N_f is the number of quark flavors involved, M is the effective momentum scale in the matter and Λ is the scale fixing parameter of qcd. The effective momentum scale is estimated to be:

$$m^2 = \frac{4}{3}\sum_i \frac{n_i\langle\vec{p}^2\rangle_i}{\sum_i n_i}$$

where the sum is over all the constituent species present, each with a number density n_i. $\langle\vec{p}^2\rangle_i$ is the thermal average of the three momenta of species i. In the case of massless quarks, the above formula reduces to:

$$m^2 = \frac{4/3(16\int_0^\infty dpp^4N_p + 6\sum_f \int_0^\infty dpp^4n_p)}{16\int_0^\infty dpp^2N_p + 6\sum_f \int_0^\infty dpp^2n_p}$$

where

$$n_p = \frac{1}{e^{(P-\mu)/T}+1} + \frac{1}{e^{(P+\mu)/T}+1}, \qquad N_p = \frac{1}{e^{P/T}-1}$$

We have evaluated the Bose integrals by the identity:

$$\int_0^\infty \frac{z^{x-1}}{e^z-1}\,dz = \Gamma(x)\zeta(x) \qquad x>1$$

where Γ is the factorial function and ζ the Riemann zeta function. Fermion integrals must be approximated for arbitrary chemical potential and temperature.

$$m^2 = \frac{4}{3}\,\frac{(16\cdot 4!\zeta(5)T^5+6\sum_f\int_0^\infty dpP^4n_p)}{(16\cdot 2\cdot\zeta(3)T^3+6\sum_f\int_0^\infty dpP^2n_p)}$$

The special case of T=0 is the well known result:

$$m^2 = \frac{4}{5}P_F^2$$

The quark thermodynamical potential is given as a function of the chemical potential and temperature up to third ordering ($g=\alpha/4\pi$) by Kapusta.[1]

$$-\Omega = P = \frac{8\pi^2}{45}T^4 + \frac{7\pi^2}{60}n_fT^4$$

$$+ n_f\left(\frac{1}{4\pi^2}\mu^4 + \frac{1}{2}T^2\mu^2\right) - g^2\left(\frac{T^4}{6} + \frac{5n_fT^4}{72} + \frac{1}{8}n_f\left(\frac{\mu^4}{\pi^4} + \frac{2\mu^2T^2}{\pi^2}\right)\right) +$$

$$\frac{2}{3}\frac{g^3}{\pi^4}T\left(\pi^2T^2 + \frac{1}{2}\sum_f\int_0^\infty\frac{dp}{E_p}n_p(p^2+E_p^2)\right)^{3/2}$$

On the other hand, a nonlinear relativistic field theory is being used to describe nuclear matter at densities and temperatures below the nuclear-quark matter phase transition. Then we do phase equilibrium.

In summary, calculations of transition curve for nuclear-quark gluon plasma are being done by using a perturbative qcd expansion of the quark pressure and a nonlinear relativistic field theory for nuclear matter.

---

1. J. Kapusta, Nucl;. Phys. B148, 461 (1979).

SENSITIVITY OF COLLECTIVE NUCLEAR MATTER FLOW TO THE EQUATION OF STATE

G. Buchwald*, G. Graebner*, M. Uhlig*,
D. Barthel*, J.A. Maruhn*, W. Greiner*,
J. Theis**, and H. Stöcker

Nuclear collisions at high energy offer the unique opportunity to explore properties of excited matter. In particular they allow the investigation of the nuclear equation of state $E_c(\rho)$. One tool for doing this is the analysis of the collective nuclear matter flow resulting from a high energy heavy ion collision. This "global" momentum tensor analysis[1] can be done in 4π detector systems like emulsions, streamer chambers, or the plastic ball. The basic idea is to measure on an event-by-event basis simultaneously all particles and all the associated momenta. Once this information is available, one can transform the physical quantitites into the center-of-momentum frame and determine the direction of maximum momentum and energy flow by performing a principal axis transformation. One possible concept proposed to analyze nuclear collisions is the kinetic flow tensor[1]:

$$F_{ij} = \frac{1}{N} \sum_{\nu} \frac{p_i(\nu) p_j(\nu)}{2m(\nu)} \qquad (1)$$

which gives the principal axes of the kinetic energy flow.

The most important observables from this analysis are the flow angle $\theta = \arccos([Q_3]_z/Q_3)$ and flow ratio $R_{1/3}=Q_1/Q_3$ with $Q_1>Q_2>Q_3$ the principal values of the flow tensor.

We have calculated the flow tensor resulting from hydrodynamical model calculations at b=0 and found a strong dependence of the flow ratio ($R_{1/3}$) excitation function on the nuclear equation of state. Fig. 1 shows a strong enhancement of $R_{1/3}$

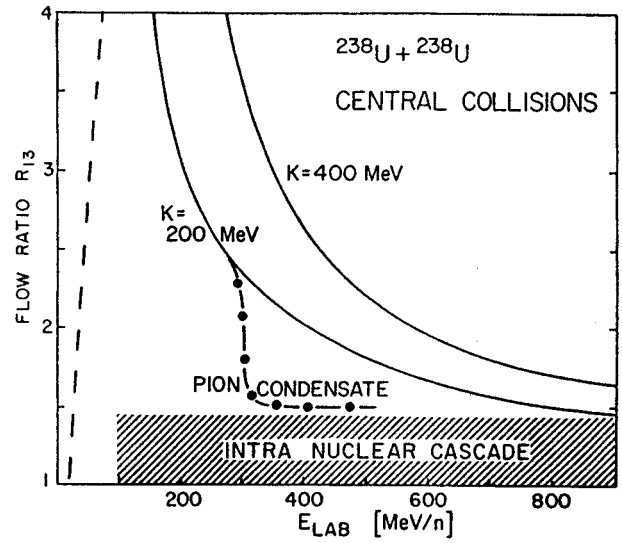

Fig. 1. Dependence of the $R_{1/3}$ excitation function on the shape of the nuclear equation of state.

at intermediate and low energies $E_{Lab}<300$ MeV/n, where the reaction becomes more sensitive to the collision dynamics. Here, owing to lower temperatures thermal effects are weaker and therefore collective flow effects resulting from nuclear properties and reflecting the equation of state become more important. For the compression constant K=200 MeV (full line) and $E_c(\rho)\sim\rho$ for $\rho>>\rho_0$ $R_{1/3}$ is approximately constant for $E_{Lab}\gtrsim 400$ MeV, whereas for $E_{Lab}<400$ MeV a drastic increase with decreasing E_{Lab} can be observed. K=400 MeV (broken line) yields the same limit for high E_{Lab}, but the enhancement for low energies is even greater than for K=200. This is reasonable because at higher compressibility nuclear matter is pressed to the side much more strongly, resulting in a larger $R_{1/3}$. With K=400 and $E_c(\rho)\sim\rho^2$ for $\rho>>\rho_0$ this feature is even more pronounced and further the limiting $R_{1/3}$ for high E_{Lab} is larger than in the previous two cases. Thus Fig. 1 shows that it seems to be possible to obtain information about the nuclear equation of state by measuring the $R_{1/3}$ excitation function at energies below $E_{Lab}\sim 600$ MeV/n.

---

* Universitat Frankfurt

** GSI Darmstadt

1. M. Gyulassy, K. Frankel, H. Stöcker, Phys. Lett. 110B, 1982; H. Stöcker, G. Buchwald, C.P. Csernai, G. Graebner, J.A. Maruhn and W. Greiner, Nucl. Phys. A387, 205c (1982).

COMPARISON OF HYDRODYNAMICAL CALCULATIONS WITH RECENT CERN $^{12}C(184\ MeV/n)+^{197}AU$ PROTON DATA

G. Buchwald*, G. Graebner*, J.A. Maruhn*,
W. Greiner*, J. Theis**, H. Stöcker

Viscous three dimensional fluid dynamical calculations are performed for the reaction $^{12}C + ^{197}Au$ at 84 MeV/n. In order to obtain inclusive cross sections which can be compared with experimental data, fluid dynamical calculations are made for impact parameters b=1;3;5;7 fm. Subsequently a subroutine assuming local thermal and local chemical equilibrium is attached[1] to each run. The resulting cross sections are averaged over all impact parameters.

Figure 1 shows the fluid dynamical results compared with the data of Jakobsson et al.[2] The calculations are in qualitative agreement with the data. Thre are two points, however, which require further discussion. First the experimental data seem to indicate a dip at energies around 50 MeV which does not occur in the calculations. But comparison with other data[3] seems to show that this point is not settled experimentally. Second the absolute value of the calculational results is a factor 6-6 too small. Most of this is due to the fact that the chemical equilibrium model used here does not take into account the decay of excited reaction products into protons. The additional amount of protons stemming from this mechanism can be estimated to shift our results by a factor 4-5.[4] Thus improved calculations now in progress promise to yield much better agreement between data and theory. Selecting to central events the fluid dynamical model predicts a strong forward suppression of the cross section. This can be seen most impressively in the α cross section (Fig. 2) because the α's are formed preferentially in the colder reaction zones.[1] Therefore their cross section is smeared out least by thermal motion and retain a large amount of collective flow information.

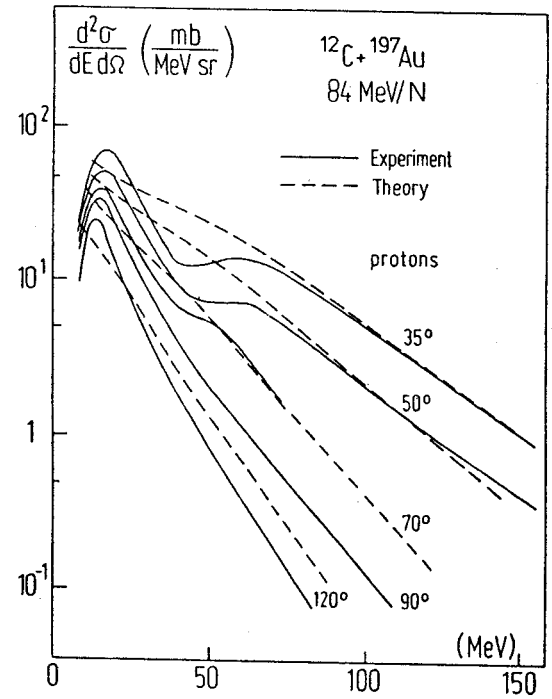

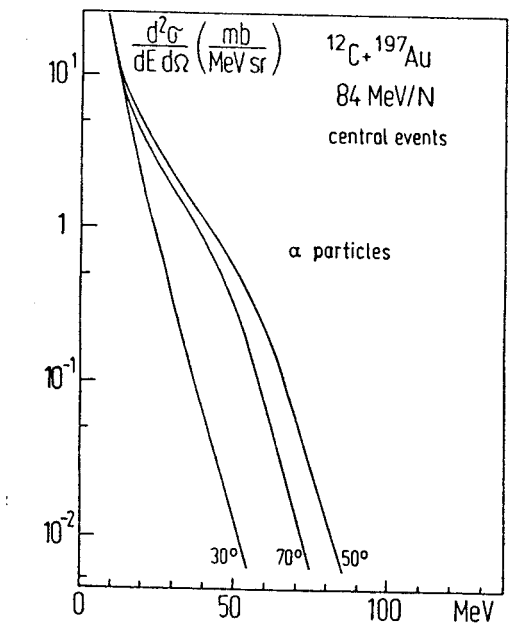

* University of Frankfurt
** GSI Darmstadt

1. G. Buchwald, G. Graebner, P.R. Subramaniar L.P. Csernai, J. Theis, J.A. Maruhn, W. Greiner and H. Stöcker, Proc. of the XX Intl Winter Meeting on Nuclear Physics, Bormic Italy, Jan. 25-30, 1982, p. 734 and refs. therein.
2. B. Jakobsson et al., Phys. Lett. 102B, 121 (1981) and Univ. of Lund, preprint LUIP 8208 June 1982.
3. R. Glasow et al., GSI report 82-1, p. 35.
4. H. Stöcker, private discussion and G. Buchwal et al., UFTP preprint 95/1982, to be published.

DOUBLE SHOCKS IN RELATIVISTIC NUCLEUS NUCLEUS COLLISIONS

G. Graebner*, J.A. Maruhn*, W. Greiner*,
H. Stöcker and H. Kruse

Although the existence of shock waves in the region of a phase transition in nuclear matter has been discussed a number of times,[1-4] there are still interesting aspects to be investigated. In particular, the question arises whether a density isomer in nuclear matter reveals a characteristic signature in the behavior of shock waves, e.g. the appearance of double shocks.

We have investigated a schematic equation of state (EOS) for nuclear matter (Fig. 1) with a second minimum at relatively high density. The

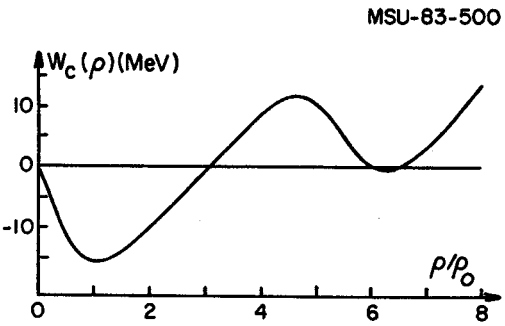

Fig. 1. Compressional energy per particle as a function of density.

thermal energy is taken to be that of a nonrelativistic Fermi gas. In the schematic shock model, a slab symmetry is assumed for two colliding nuclei and the relativistic Rankine-Hugoniot equation is solved for the state variables behind the shock front(s). The density and temperature behind a single shock wave are shown as a function of bombarding energy by the solid lines in Fig. 2. In the region indicated by the arrows, a single shock wave is not stable because the shock velocity, β_s, decreases as a function of density. Here one finds two shock waves.[5] The first compresses the matter to the state corresponding to the local β_s maximum, indicated by the lower dashed line in Fig. 2, and is followed by a second shock wave which compresses the matter from this intermediate state to the isomeric state indicated by the upper dashed line. For a given bombarding energy, this double shock configuration is stable, with growing spatial regions of intermediate as well as isomeric density if the second shock does not overtake the first. Note that such a double shock exists as well if the Maxwell construction is used in the phase transition region because β_s still decreases with ρ.

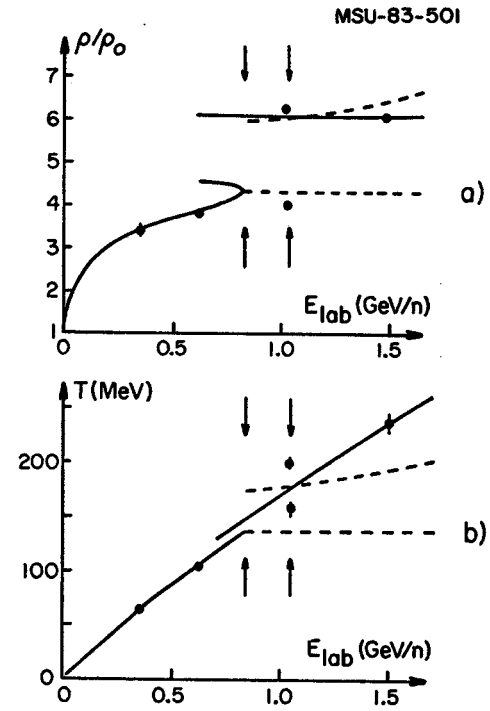

Fig. 2. Density (a) and temperature (b) after single shock (solid line) and double shock (dashed line). Arrows delimit double shock region and points are fluid dynamical solutions.

In addition to the schematic shock model, the relativistic fluid dynamical equations were solved numerically in one dimension for this EOS. The values of ρ and T behind the shock front are in excellent agreement with the shock model, as indicated in Fig. 2. In particular, the double shock configuration, with growing regions of both densities, is found in an appropriate energy region.

The density and temperature behind the second shock front are considerably higher than behind the first. However the doubly shocked zone represents only a fraction of the matter present so that the experimental manifestation of the double shock will be a smearing out of threshold phenomena, e.g. pion emission, associated with a density isomer.

* University of Frankfurt

1. J. Hofmann, H. Stöcker, U. Heinz, W. Scheid, and W. Greiner, Phys Rev. Lett. 36, 88 (1976).
2. V.M. Galitskii and I.N. Mishustin, Phys. Lett. 72B, 285 (1978).
3. J. Hofmann, B. Müller, and W. Greiner, Phys. Lett. 82B, 195 (1979).
4. H. Kruse, W.T. Pinkston, and W. Greiner, J. Phys. G8, 567 (1982).
5. G.E. Duvall and R.A. Graham, Rev. Mod. Phys. 49, 523 (1977).

PHASE TRANSITION OF THE NUCLEON-ANTINUCLEON PLASMA IN A RELATIVISTIC MEAN FIELD THEORY

J. Theis*, J. Polonyi*, H. Stöcker
G. Graebner**, G. Buchwald**, M. Uhlig**,
J.A. Maruhn** and W. Greiner**

We study Walecka's mean field theory[1] with the following results: i) We can reproduce the observed binding energy and density of nuclear matter within experimental precision in an area characterized by a line in the coupling plane Fig. 1). The coupling constant values proposed

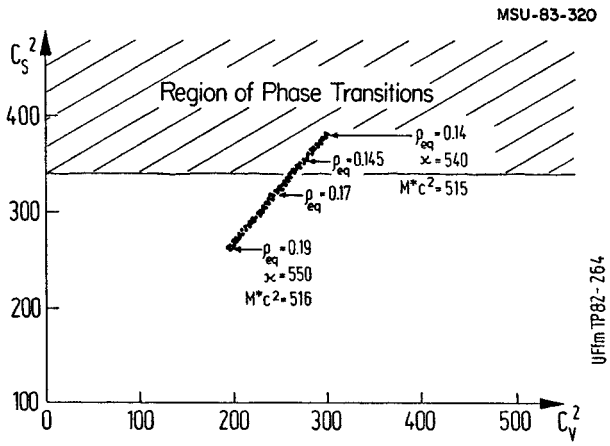

Fig. 1. The coupling constant plane is shown.

by Walecka represent a point close to the end of this line. ii) We have found that part of this line defines systems which exhibit a phase transition around $T_c \sim 200$ MeV for zero baryon density. The rest of this line corresponds to such systems where the phase transition is absent but there is a peak in the specific heat around $T \approx 200$ MeV.

Phase structure: we explore the phase structure for the effective Lagrangian

$$L = L^{free}_{Dirac} + L^{free}_{\phi} + L^{free}_{v_r} + g_s\phi\bar{\psi}\psi + ig_v V^{\mu}\bar{\psi}\gamma_{\mu}\psi$$

at vanishing chemical potential μ and vector density ρ. In contrast to $\mu \neq 0$, the Fermi integration can be done analytically yielding for the total energy density

$$e = \frac{1}{2\zeta^2}(\lambda - x)^2 + \frac{\gamma\theta x^3}{\pi^2}\sum_{n=1}^{\infty}\frac{(-1)^{n-1}}{n}\{K_1(nx/\theta) + \frac{3\theta}{nx}K_2(nx/\theta)\} \qquad (1)$$

for the pressure

$$p = -\frac{1}{2\zeta^2}(\lambda - x)^2 + \frac{\gamma\theta x^2}{\pi^2}\sum_{n=1}^{\infty}\frac{(-1)^{n-1}}{n^2}K_2(nx/\theta) \qquad (2)$$

and for the effective mass

$$x = [\lambda + \frac{\gamma\zeta^2\theta x}{\pi^2}\sum_{n=1}^{\infty}K_2(nx/\theta)\frac{(-1)^{n-1}}{n}]^{-1} \qquad (3)$$

here γ is the degeneracy factor. θ defines the dimensionless temperature $\theta = T/Mc^2$. K_1 and K_2 stand for the modified Bessel-functions of first and second order, respectively. Fig. 2 contains the solution x of the self consistency equation

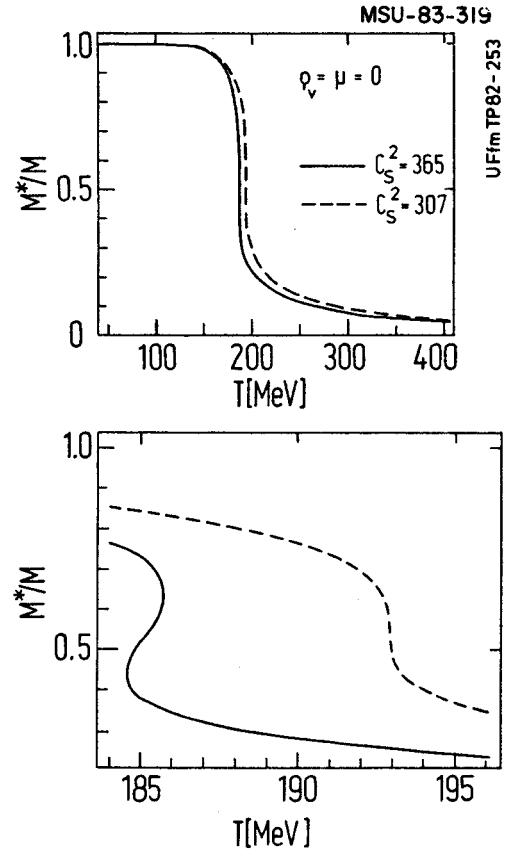

Fig. 2. The effective mass is shown as a function of temperature for different C_s^2-values.

(3) as a function of the temperature. The general trend of the function x(θ) can be understood as follows: The scalar density, which appears as a source for the scalar meson field ϕ, increases with increasing temperature. This leads to an increase of the mean field value of ϕ. Since the scalar meson describes an attractive interaction of the nucleons, these will be bound more strongly, and thus the effective mass is reduced. This mechanism is reinforced by the fact that a decrease of the effective mass increases the scalar density again. The most striking feature is the sudden drop in x at temperature $T \approx 200$ MeV where the transition from x=.9 to x=.1 occurs in

an interval of $\Delta T \sim 2$ MeV only. We calculated the thermodynamical quantities for the various coupling constants of the region shown in Fig. 1. For $C_s^2 > 342$ we found a phase transition of first order. For $C_s^2 < 342$ the thermodynamical behavior is smooth in the temperature but a peak of finite width is found in the specific heat. For $C_2^2 = 342$ there is a phase transition of second order. Thus we have an effective theory in which the order of the phase transition directly depends on the strength of the coupling constant.

* GSI Darmstadt
** Universitat Frankfurt
1. J.J. Walecka, Phys. Lett. 59B, 109 (1979).

SYSTEMATICS AND PREDICTION OF CROSS SECTION IN DEEPLY INELASTIC AND FRAGMENTATION REACTIONS

A.D. Panagiotou*, B. Sherrill, W. Benenson and D.K. Scott

The production cross section of heavy fragments in Deeply Inelastic Rections (DIR) at $E/A \leq 15$ MeV and in Fragmentation Reactions (FR) at $E/A \geq 25$ MeV, exhibits similarities and systematics, which have been the center of intensive investigation (1,2 and references therein):

1. Analysis of experimental data for both types of reactions shows that the emission of fragments occurs on a similar time scale of ~ 10^{-22} sec.
2. The most probable kinetic energy of the fragments - in the system of the decaying excited nucleus - is indepentent of the type and bombarding energy of the primary particles. It is approximately determined by the exit Coulomb barrier.
3. An increase in the width of the fragment energy is observed with increasing excitation energy of the decaying nuclei.
4. In both processes the final systems have continuous excitation energy spectrum. The maximum excitation energy is well defined only in DIR.
5. In both processes, apart from the fragment and the residual nucleus in the final state, only a few light particles are emitted.
6. The isotope distribution in both processes exhibits an odd-even neutron-number effect, reminiscent of the binding energy per nucleon.
7. The cross section at forward angles (< grazing angle) is dominated by quasi-elastic transfer (projectile fragmentation) at low (high) incident energies.
8. In both processes, the centroid of the isotope yield distribution peaks at R ~ 1, where R=(N/Z)ejectile/(N/Z)projectile.

The possibility of acurately predicting the cross section of yet unobserved neutron-rich nuclei is of current interest, in view of the continuing attempts to investigate the region further away from the valley of stability.

Taking into account the above observations, we fitted the isotope distributions from both DIR (3-5),and FR (6,7) with the expression:

$$Y(N) = C \exp\{-A[R+(1-BE/BEmx)]-Q/T\} \qquad [1]$$

where C is the normalization constant,

A is the mass number of the isotope A=N+Z,

R=(N/Z)ej./(N/Z)pr.,

BE is the binding energy per nucleon of each isotope,

BEmx is the maximum binding energy per nucleon of the fitted isotopes,

Q is the binding energy of the emitted fragment in a binary breakup of the projectile for FR, or the reaction Q-value for DIR, and

T is a quantity related to the excitation of the system.

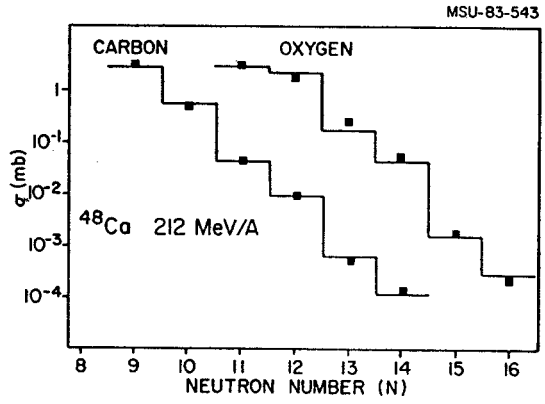

Fig. 1. The fit (hystogram) of expression [1] to FR isotope production cross sections from the reaction 48Ca + 9Be at 212 MeV per nucleon (6,7).

Figure 1 shows typical fits of the above relation to the isotope distributions, obtained in the fragmentation of 48Ca at 212 MeV/A (6,7). We observe that the odd-even effect and the relative cross section is quite well reproduced, within the assumed 15% experimental error. It should be noted that the production cross sections span, in some cases, over four orders of magnitude.

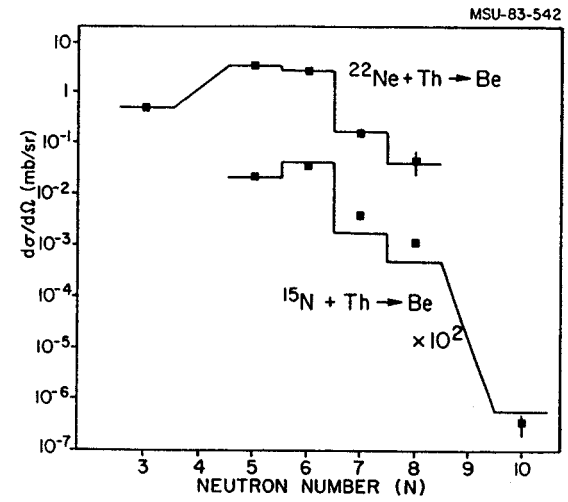

Fig. 2. The fit (hystogram) of expression [1] to DIR isotope production cross sections (3,4).

Figure 2 shows the fit of expression [1] to isotope production cross sections. obtained in DIR (3,4). Again the cross section is well reproduced within the experimental error. These fits can be extrapolated to obtain production cross sections for new more neutron-rich and yet unknown isotopes.

It is planned to check the predictive power of this simple expression by doing measurements in the Recoil Particle Mass Separator of the NSCL.

* Permanent address: Physics Department, University of Athens, Athens Hellas

1. V.V. Volkov, Phys. Rep. 44C (1978) 94
2. V.V. Avdeichikov, Phys. Lett. 82B (1980) 74
3. A.G. Artukh, G.F. Gridnev, V.L. Mikheev and V.V. Volkov, Nucl. Phys. A283 (1977) 350
4. A.G. Artukh,
5. V.V. Volkov et al, Preprint J.I.N.R. Dubna, 1979
6. G.D. Westfall, et al, Phys. Rev. Lett. 43 (1979) 1859
7. J.D. Stevenson and P.B. Price, Phys. Rev. C24 (1981) 2102

EVIDENCE FOR LIQUID-GAS PHASE TRANSITIONS IN HOT NUCLEAR SYSTEMS

A.D. Panagiotou*, M.W. Curtin, H. Toki,
D.K. Scott and P.J. Siemens[$]

In high energy proton-nucleus and nucleus-nucleus collisions, hot nuclear matter could exist as a two-phase liquid-gas mixture. Phase transition phenomena may occur, manifesting themselves most probably in the formation of intermediate mass fragments.

The possibility of phase transition in an equilibrated system was previously considered theoretically in a number of papers (1-5 and ref's therein). It has also been suggested in a number of recent papers (6-8), that the power law dependence: $Y(A) \sim A^{-\tau}$ of the fragment distributions may constitute a signature for the occurrence of phase transition phenomena near a critical point. The widely differing systems, which exhibit this characteristic power law dependence, suggest that phase transitions are global in origin, dependent only on the energy imparted to the system and not on the details of the reaction. We report on the analysis of the available intermediate-mass fragment data using : i) a power law dependence, and ii) a modulated power law, taking into account the temperature dependent surface and volume free energies and chemical potential energy. We follow Fisher's theory of condensation (13), for the system of hot nuclear matter. The probability for fragment (droplet) formation of size A is given by the expression:

$$P(A) \sim A^{-k} \exp\{[-a_s'(T)A^{2/3} - a_v'(T)A + \mu(T)A]/T\}$$

where k is the critical exponent, $a_s'(T) = a_s(T) - TS_s$ is the surface free energy per particle, $a_v'(T) = a_v(T) - TS_v$ is the volume free energy per particle and $\mu(T)$ is the chemical potential per particle.

Relation (1) can be written in the following form:

$$P(A) \sim A^{-k}\, X^{**}(A^{2/3})\, Y^{**}A$$

where:

$$X = \exp[\, -a_s'(T)/T\,]$$

$$Y = \exp\{-[\, a_v'(T) - \mu(T)\,]/T\}$$

We distinguish the following three regions :

I. T < Tc. The Liquid - Gas Coexistance Region

In this region the sum of the volume energy per particle in the liquid phase and the Gibbs free energy per particle in the gaseous phase is equal to zero, $[a_v'(T) - \mu(T)] = 0$. Therefore, the exponential factors are Y = 1 and X < 1, and the probability P(A) can be written as:

$$P(A) \sim A^{-k} \exp\{-[\, a_s'(T)\, A^{2/3}\,]/T\,\} \quad (1)$$

II. T = Tc. The Critical Point

Here the surface free energy term is equal to zero : $a_s'(T) = 0.$ and in addition, $[a_v'(T) - \mu(T)] = 0$. Therefore, both exponential factors are X = 1 and Y = 1, and the probability assumes the pure power law:

$$P(A) \sim A^{-k} \quad (2)$$

III. T>Tc. The Gaseous Phase Region

In this region we assume that the surface free energy remains zero, $a_s'(T) = 0.$, while, $[a_v'(T) - \mu(T)] > 0$. Therefore, the exponential factors are X = 1 and Y < 1, and the probability P(A) assumes the form:

$$P(A) \sim A^{-k} \exp\{-[a_v'(T) - \mu(T)]A/T\} \quad (3)$$

We notice that the exponential factors X and Y, at temperatures T < Tc and T > Tc respectively, modulate the pure power law dependence of the fragment distribution.

To understand the temperature dependence of the data, we fitted the available fragment distributions (6-12), with a power law dependence of the form: $P(A) = C.\ A^{-\tau}$, where τ is the "apparent" exponent. In this approximation, for T =/ Tc, we include in the power exponent, τ , the effects of the exponential factors X and Y. We, therefore, expect this apparent exponent to vary with temperature. In fig. 1 we plot the apparent exponent, τ, of the power law least squares fit to the fragment distributions versus the emitting system's temperature, T. We observe a dramatic

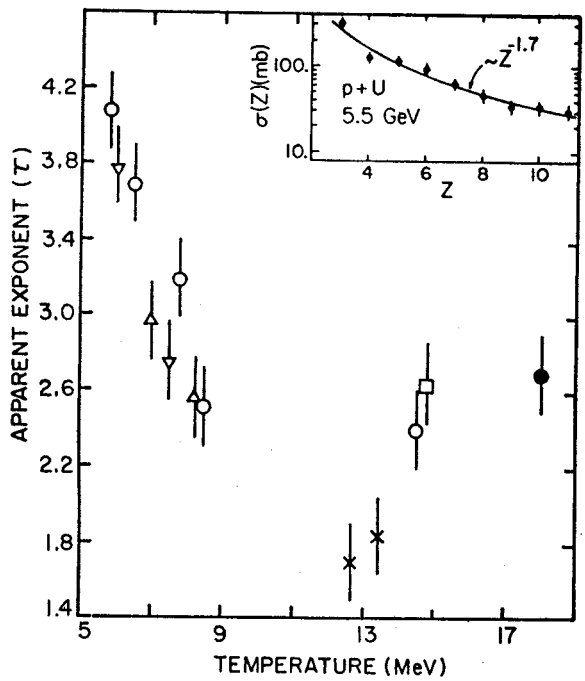

Fig. 1. The apparent exponent, τ, of the power law fit to the fragment distributions as a function of the system's temperature, T.

temperature dependence of the apparent exponent. At temperatures lower than about 11 MeV the apparent exponent increases quickly as the temperature decreases, while for temperatures higher than 11 MeV it increases again with increasing temperature. The exponent appears to assume its smallest value of about 1.7 at a temperature of about 11 MeV. If we assign the

critical temperature, Tc, corresponding to the lowest value of the apparent exponent, i.e, corresponding to the maximum probability for fragment emission, then from fig. 1 we conclude that Tc ~ 11 MeV.

Some comments should be made at this point:

1. The pure power law exponent, (τ = k of expression (2) at T = Tc), assumes a value lower than 2.0, a minimum value for an infinite system.

2. The indication from experimental data of a critical temperature at Tc ~ 11 MeV is in strong dissagreement with the suggestion that Tc = 3.3 MeV (14), or Tc ~ 18 MeV as estimated from nuclear matter calculations (21). Fig. 2 shows the dependence of the apparent exponent, τ, of the power law fit to the fragment distribution, on the incident kinetic energy for the systems (p+Ag), (p+Kr,Xe). We observe again, in the absence of the uncertainty on the temperature of the system, that the apparent exponent decreases monotonically with increasing energy, up to an energy of about 2-4 GeV and then it levels off, approaching a limit at very high energies. We may associate the turning point of the curve at the minimum value of the apparent exponent with the critical point of fig. 1.

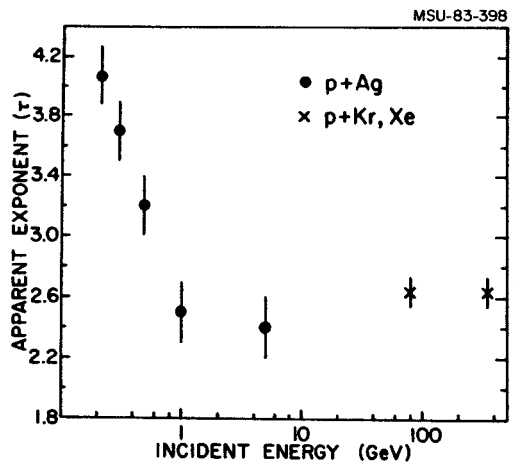

Fig. 2. The apparent exponent, τ, of the power law fit to the fragment distributions for the systems (p+Ag), (9,10,11), and (p+Kr,Xe), (6), as function of the incident energy.

The dramatic features of the temperature dependence of the fragment yield distribution, prompted us to fit again the fragment distributions with expressions (1) and (3) for T < Tc and T > Tc, respectively. We empirically parameterised the temperature dependence of the surface free energy as:

$a_s'(T) = 18.4\ (1 - T/Tc)^2 \qquad T < Tc$

since: as'(T=0) = 18.4 MeV, the cold nuclear matter surface energy, and $a_s'(T=Tc) = 0$, as T approaches Tc. Similarly, for the volume and Gibbs free energies we take:

$a_v'(T) - \mu(T) = b\ (1 - T/Tc)^2$ for T > Tc

where $(8 \leq b \leq 10)$

We least-squares fit the fragment distributions with:

$(P(A) = C.A^{-k} \quad \exp\{[-as'(T)A^{2/3} \quad /T\}\ T<Tc)$

$(P(A) = C.A^{-k} \quad \exp\{-[av'(T) - \mu(T)]A/T\}\ T>Tc)$

letting the exponent, k, take successively the values 1.6, 1.7, 1.8, 2.0, 2.33 and obtained the corresponding Tc-values. For the temperature of the system we used T = T' +/- 1. MeV, where T' is the temperature over all emitted fragments used in the fit.

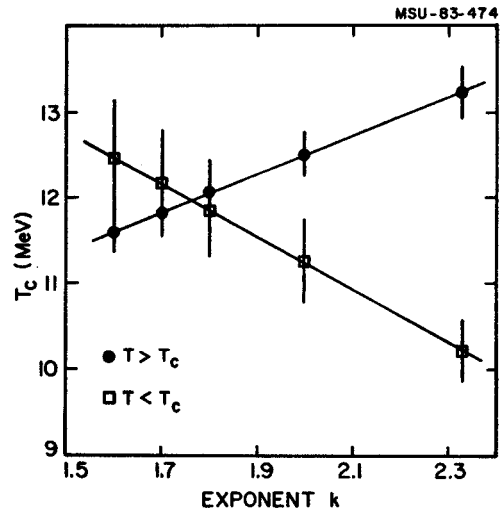

Fig. 3. The extracted critical temperature, Tc, as a function of the critical exponent, k, for T < Tc and T > Tc.

Figure 3 shows the extracted critical temperature as a function of the exponent, k. We observe that for $1.7 \leq k \leq 1.8$ the calculated Tc-values coincide for both T < Tc and T > Tc, while for both lower and higher k-values they diverge. We are, hence, inclined to accept k ~ 1.7 as the critical exponent and Tc = 12.2 +/- 0.2 MeV as the critical temperature.

Sauer, Chandra and Mosel,(17), calculated the thermal properties of nuclei, using the thermal Hartree-Fock aproximation and the Skyrme III interaction and obtained a critical temperature Tc = 12.58 MeV for the liquid drop surface free energy. Our extracted critical temperature, from the fit to the experimental fragment distributions, is in aggreement with their theoretical value.

* Permanent Address: Department of Physics, University of Athens, Athens, Hellas
$ Texas A&M University, College Station, Texas 77605

1. P. Danielewicz, Nucl. Phys. A314 (1979) 465
2. H. Schulz, L. Munchow, G. Ropke, M. Schmidt, Phys. Lett. 119B (1982) 12
3. M.W. Curtin, H. Toki, D.K. Scott, Phys. Lett. 123B (1983) 289
4. H. Jacaman, A.J. Mekjian, L. Zamick, Preprint RU- 83-61
5. P.J. Siemens, to be published in Nature
6. J.E. Finn et al, Phys. Rev. Lett. 49 (1982) 1321
7. H.H. Gutbrod, A.I. Warwick, H. Wieman, Nucl. Phys. A387 (1982) 177c
8. C.B. Chitwood, D.J. Fields, C.K. Gelbke, W.G. Lynch, A.D. Panagiotou, M.B. Tsang, H. Utsunomiya, W.A. Friedman, to be published in Phys. Lett.
9. R.E.L. Green, R.G. Korteling, Phys. Rev. C22 (1980) 1594
10. E.N.Vol'nin, A.A. Vorob'ev, D.M. Seliverstov, JETP Lett. 19 (1974) 357
11. G.D.Westfall, R.G.Sextro, A.M.Poskanzer, A.M.Zebelman, G.W.Butler, E.K.Hyde, Phys. Rev. C17 (1978) 1368
12. A.M. Poskanzer, G.W. Butler, E.K. Hyde, Phys. Rev. C3 (1971) 882
13. M.E. Fisher, Physics 3 (1967) 255
14. R.W. Minich et al, Phys. Lett. 118B (1982) 458
15. A. Mekjian, Phys. Lett. 89B (1980) 177, and references therein
16. M.-C. Lemaire, S. Nagamiya,S. Schnetzer,H. Steiner and I. Tanihata, Phys. Lett. 85B (1979) 38
17. G. Sauer, H. Chandra and U. Mosel, Nucl. Phys.A264 (1976) 221

EXPERIMENTAL DETERMINATION OF THE ENTROPY FROM THE α TO PROTON RATIO

M.W. Curtin , H. Toki and D.K. Scott

In relativistic heavy ion collisions, it has been suggested that entropy remains essentially constant during the disassembly process[1]. If this assumption is valid and the entropy can be related to experimental observables, the entropy of the primary "fireball" can be ascertained. One method suggested[2] is to examine the deuteron to proton ratio, R_{dp}. To see how R_{dp} is related to the entropy we make the following assumptions:

1) The binding energy of the deuteron (E_B ~ 2.225 MeV) is approximately zero.

2) The number of protons is approximately the same as the number of neutrons i.e. $N_p \approx N_n$.

3) The number of deuterons is small compared to the number of protons ($N_d << N_p$) and furthermore for all heavy fragments $N_{A>>} << N_p$. The proton, neutron and deuteron chemical potentials obey the following relations for equilibrium:

4) $\mu_p + \mu_n \approx \mu_d$

5) $\mu_p \approx \mu_n$

If the ideal gas approximation is valid, the chemical potential is known from elementary thermodynamics[3] to be of the form:

$$e^{\mu_j/T} = \frac{N_j}{V} g_j^{-1} \left(\frac{2\pi\hbar^2}{M_j T}\right)^{2/3} e^{F_j/T} \qquad (1)$$

where

μ_j = chemical potential of species j

g_j = degeneracy of species j

$= 2S_j + 1$

F_j = free energy of species j

$= E_j - TS_j$

If we assume only the ground state (T=0) deuteron is observed and ignore the binding energy of the deuteron as per assumption 1, the free energy is zero. Hence,

$$R_{dp} = \frac{N_d}{N_p} = \frac{g_d}{g_p}\left(\frac{M_d}{M_p}\right)^{2/3} e^{(\mu_d - \mu_p)/T}$$

$$= \frac{3}{2}\,(2)^{3/2}\, e^{\mu_p/T} \qquad (3)$$

The Sakur-Tetrode relation for a monatomic ideal gas is

$$S_j = \frac{5}{2} N_j - N_j \frac{\mu_j}{T} \qquad (4)$$

Thus the total entropy of a deuteron-proton-neutron gas mixture is

$$S_{tot} = \sum_j S_j$$

$$= \frac{5}{2}\,(N_p + N_n + N_d) - \frac{(2\mu_p N_p + \mu_d N_d)}{T}$$

$$\frac{S_{tot}}{N} \sim \frac{5}{2} - \frac{\mu_p}{T} \qquad (5)$$

Utilizing the result of equation 3, we deduce

$$\frac{S_{tot}}{N} \sim 3.95 - \ln R_{dp} \qquad (6)$$

Examination of Table 1 indicates that as the incident energy of the projectile decreases, hence resulting in a lower temperature of the emitting system, the assumption $N_{A>>} << N_p$ is not fulfilled. The α production increases relative to the lighter masses for T ≤ 20 MeV and actually exceeds the production of lighter composite fragments at T ~ 7 MeV. At extremely low temperatures, the α production cross section exceeds the proton cross section.

It is interesting to develop an expression for the lower temperatures based on similar reasoning. In the interest of simplicity, ideal gas relations are also used despite the fact that one should in principle use the Fermi-Dirac and Bose-Einstein statistics for temperatures less than the Fermi Energy.

The binding energy of an α particle (≃ 27 MeV) is far greater than the binding energy of a deuteron and hence should not be ignored. The number of α particles is assumed large compared to all composite fragments, however it is not assumed small compared to the proton production cross section.

Similarly we find

$$N \sim 2 N_p + 4 N_\alpha$$

$$R_{\alpha p} = \frac{N_\alpha}{N_p} \sim \frac{1}{2} \cdot (4)^{3/2} \cdot e^{(4\mu_p - E_\alpha - \mu_p)/T}$$

$$= 4\, e^{(3\mu_p - E_\alpha)/T}$$

$$\frac{S_{tot}}{N} \sim \frac{5}{2} - \frac{1}{3}\ln\left(\frac{R_{\alpha p}}{4}\right) - \frac{15}{2}\left(\frac{R_{\alpha p}}{2 + 4 R_{\alpha p}}\right) + \frac{27}{T}\left[\frac{R_{\alpha p}}{2+4R_{\alpha p}} - \frac{1}{3}\right]$$

Inserting average values of the temperatures and the α to proton ratio, the results are presented in Table 1. It is interesting to compare the results in the high energy region where the assumption of N_α greater than all other composites breaks down, with the hydrodynamical predictions[4]. The results are quite similar.

Table 1. The incident energy, projectile and target are indicated in the first column. The average extracted temperatures for light fragments and the measured α to proton ratios are shown. The deduced entropy per nucleon is reported in the last column.

Einc ($\frac{MeV}{u}$)	T	$R_{\alpha p}$	S/N
8.8 (^{16}O+ ^{197}Au)	3.4	1.83	.20
13.4 (^{16}O+ ^{197}Au)	5.0	1.0	.81
20 (^{16}O+ ^{197}Au)	7.0	0.5	1.45
35 (^{12}C+ ^{197}Au)	10.72	.3	2.05
100 (^{20}Ne+ ^{197}Au)	21.65	.23	2.53
150 (^{20}Ne+ ^{197}Au)	27.5	.18	2.78
241 (^{20}Ne+ ^{238}U	32.5	.06	3.39
393 (^{20}Ne+ ^{238}U)	42.75	.068	3.44
790 (^{12}C+ ^{197}Au)	71.0	.032	3.88

1) H. Stoecker et al., Michigan State University Cyclotron Preprint No. 399 (1983).
2) K. van Bibber et al., Phys. Rev. Lett. 43 (1979) 840; K.A. Fraenkel and J.O. Stevenson, Phys. Rev. C 23 (1981) 1511.
3) C. Kittel and H. Kroemer, Thermal Physics (W.H. Freeman and Co., San Francisco, 1980).
4) H. Stoecker, Lawrence Berkeley Laboratory Report 12302.

THE TIME SCALE FOR A LIQUID-GAS NUCLEAR INSTABILITY

M.W. Curtin, H. Toki and D.K. Scott

The availability of heavy ion beams over a wide range of energies makes it possible to create nuclear systems with high temperatures and greater than normal nuclear densities in a laboratory environment. Such conditions may lead to phase transitions in nuclear matter conjectured to occur at greater than normal nuclear densities. It is also possible that during the process of rarefaction, following the initial compression, the system may enter a state of lower than normal nuclear density, where the conditions of temperature and density necessary for a liquid-gas coexistence may develop (1-3). If heavy ions are to be adequate probes of these states, two conditions must be satisfied: the thermalization process and the time necessary for this state to develop must be less than or of the order of the disassembly time. Firstly, we assume that the system has a sufficiently short mean free path to allow the system to equilibrate in a time commensurate with the collision time of the heavy ions. Secondly, any phase transition, for example a liquid-gas phase instability, must establish itself prior to disassembly if it is to have a discernible experimental consequence. It is important therefore to estimate the time scale for the system to disassemble and compare with the time scale necessary for the establishment of chemical equilibrium.

Time Scales Neglecting Damping

To estimate the time scale for disassembly we consider a 'mechanical' instability resulting in a breakup of the hot zone[4]. The effects of damping are neglected initially, however these effects will be taken into account in the following section. The underlying argument begins by evaluating the excitation energy per nucleon as a function of the density. Firstly, the chemical potential must be derived from the density

$$\rho = \frac{4}{(2\pi)^3} \int d^3k \left[1 + \exp\left\{\left(\frac{k^2}{2m} + E_v - \mu\right)/T\right\}\right]^{-1} \quad (1)$$

where the potential energy is obtained from the Skyrme interaction (ignoring effective mass corrections)[5]

$$\frac{E_v}{A} = -A\left(\frac{\rho}{\rho_o}\right) + B\left(\frac{\rho}{\rho_o}\right)^{5/3} \quad (2)$$

The constants A and B can be determined from nuclear matter properties in the following manner. The total energy is the sum of the thermal and potential contributions ($E = E_T + E_v$), which for T=0 has the form

$$\frac{E}{A} = \frac{3}{5}\epsilon_F\left(\frac{\rho}{\rho_o}\right)^{2/3} - A\left(\frac{\rho}{\rho_o}\right) + B\left(\frac{\rho}{\rho_o}\right)^{5/3} \quad (3)$$

where ϵ_F is the Fermi energy of normal nuclear matter ($\simeq$ 38 MeV). Nuclear matter considerations require E=-16 MeV and $\partial(E/A)/\partial\rho=0$ at $\rho = \rho_o$ and T=0. The values thus obtained are A = 74.2 MeV and B = 35.4 MeV. The thermal contribution to the energy can be calculated using

$$\frac{E_T}{V} = \frac{4}{(2\pi)^3}\int d^3k \, \frac{k^2}{2m}\left[1 + \exp\left\{\left(\frac{k^2}{2m} + E_v - \mu\right)/T\right\}\right]^{-1}$$

Utilizing thermodynamics one can calculate the entropy and pressure. The results are presented in Fig. 1, where several isentropes are plotted as a function of the density. From the initial excited compressed state formed in a heavy ion collision the system will oscillate along an isentrope in a harmonic fashion similar to a monopole oscillation in the absence of collision damping. If during the oscillation the pressure becomes positive then the system will disassociate. In practice, the incident projectiles (protons or heavy ions) are expected to create conditions of normal or greater than normal nuclear densities respectively. It is therefore necessary to define an overstressed region such that under harmonic oscillation the system will enter the region where the pressure is positive on the return portion of the oscillation. The unstable (P>0) region defines the conditions of temperature and density for which the system will disassemble and is depicted in Fig. 1.

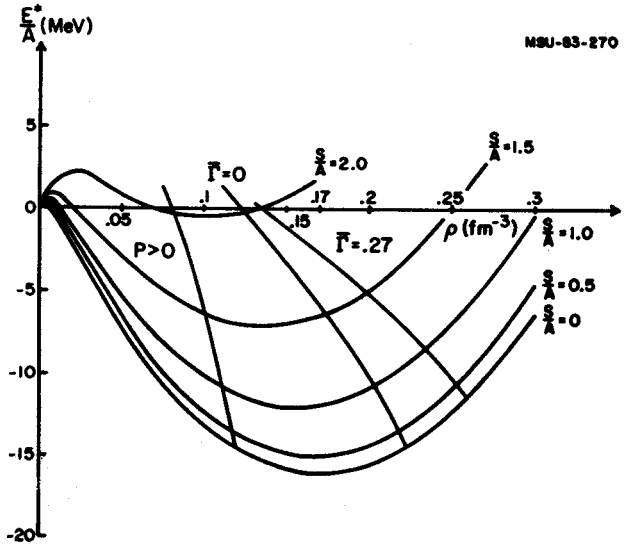

Fig. 1. The energy per nucleon versus density for various values of the entropy per nucleon. The unstable region (P>0) is indicated. This region is defined by the condition that the system will evolve or has evolved to a condition such that the pressure remains positive hence disassembling. Two boundaries for the overstressed region are drawn: No damping (labelled Γ= 0) and minimal damping (Γ= 0.27).

To understand the conditions under which the system will disassemble it is necessary to refer to figure 2 which illustrates the functional dependence of the pressure on the density. Focusing attention on the $\frac{S}{A} = 0$ isentrope it is seen that for normal nuclear density the pressure is zero as expected. Decreasing density corresponds to decreasing pressure until a maximal negative pressure point is attained whereupon the pressure increases with further decrease of the density. Once the pressure exceeds zero the pressure of the system remains positive for all further decrements in the density coordinate. Stable equilibrium is attained only when the pressure is zero and the energy is a local minimum. A system, characterized by ρ and $\frac{S}{A}$ such that it is located along the negative incompressibility portion of the isentrope (indicated in fig. 2), will move toward the lower density zero pressure point. Once the system attains zero pressure it has acquired an outward momentum and the energy is not a minimum; hence the system continues to expand until the density approaches zero. Therefore the boundary of the unstable zone is defined by successive points of maximal negative pressure for increasing isentropes.

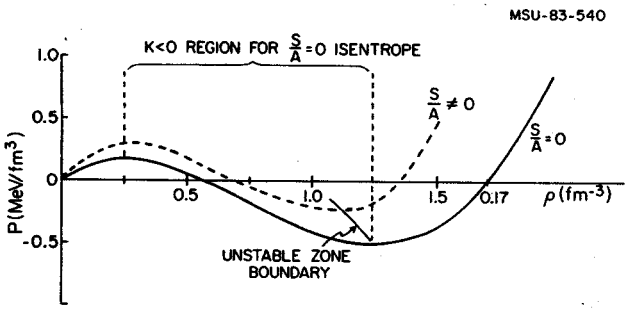

Fig. 2. Pressure versus density is plotted for $\frac{S}{A} = 0$ & $\frac{S}{A} \neq 0$ isentropes to illustrate the dynamical reasoning utilized in defining the unstable region boundary. The negative incompressibility region of the S/A = 0 isentrope is indicated to identify the portion of the isentrope for which the system will evolve to lower densities and increasing pressure until the pressure becomes positive. Since the pressure remains positive for all lower densities the system is unstable. The unstable region boundary deduced from different isentropes is plotted in Figure 1.

The system still possesses negative energy and therefore is likely to disassemble into light bound clusters. Since a deuteron is favored from entropy considerations but is severely disfavored energetically, it is most likely that the system will disassemble into slightly heavier fragments, most probably alpha particles. The boundary for the unstable region is not altered by damping considerations. In the absence of damping (Γ=0), the boundary of the overstressed region is as indicated in Fig. 1. To estimate the time required for this type of disassembly to occur we make use of the known energy of the monopole oscillations in medium mass nuclei[6]:

$$E_{monopole} \sim \hbar\omega_o \sim 15\text{MeV} \qquad (5)$$

resulting in

$$\tau_{osc} = \frac{\pi}{\omega_o} \sim 1.4 \times 10^{-22}\text{sec.} \qquad (6)$$

Estimates of the disassembly time derived from high energy cascade models give values of the order ~50 fm/c (1.7×10^{-22} sec.), consistent with the estimate from the monopole oscillation[7].

If a "chemical" instability, such as a liquid-gas phase instability, is to exist there must be sufficient time for equilibration to be established across the phase boundary. The time required for this equilibration to occur is of the same order as the evaporation time. To estimate the evaporation time we use the expression characteristic of thermionic emission[8]. Thus, the current density can be expressed as

$$J = \frac{em}{2\pi^2\hbar^3} T^2 (1-r) e^{-W/T} \qquad (7)$$

where r is the quantum mechanical reflection coefficient (taken as 0), W is the work function (taken between 8 MeV and 0 MeV) and T is the temperature. By definition

$$J = \frac{\Delta q}{\Delta t} \cdot \frac{1}{A} \qquad (8)$$

where A is the surface area of the emitting source. If we set q = e (equivalent to the emission of one nucleon) then $\Delta t = \tau_{evap}$. Assuming a spherical geometry, so that $A=4\pi R^2$ where R ~3.5 fm. as determined from the participant-spectator model for intermediate impact parameters[9] and consistent with determinations from pion interferometry measurements[10], the evaporation time is found to be

$$\tau_{evap} \sim 3.5 \times 10^{-21} \cdot \frac{1}{T^2} \cdot e^{W/T}$$

The resulting values are given in Table 1 and the W=8 MeV values are in good agreement with results deduced from an empirical fit to the measured widths of compound nuclei for A=20-100[11]. Comparing the evaporation time with the time required for disassembly it appears that for $T \gtrsim 8.1$ MeV (henceforth referred to as the breakeven temperature) the liquid-gas phase instability may develop. The range of breakeven temperatures, deduced from work functions of 0 MeV and 8 MeV, are given in Table 2 as a function of sequential evaporation times required to achieve chemical equilibrium.

Since a liquid-gas phase instability exists

only for temperatures below the critical temperature and above the breakeven temperature, it is likely that if the breakeven temperature were higher than the critical temperature the liquid-gas instability would never develop. The critical temperature of 20 MeV predicted in reference 1 assumed a binding energy per nucleon in nuclear matter of 16 MeV/u compared to the phenomenological binding energy per nucleon of 8 MeV for finite nuclei. A more thorough treatment of this question and effective mass considerations is given in reference 2, where it is shown that in finite nuclei the predicted critical temperature lies between 13.4 MeV and 8.1 MeV depending on the choice of effective mass. Thus for temperatures above 8 MeV the liquid-gas instability may develop and there is sufficient time for it to do so.

Damping Effects

Collision damping has been neglected throughout this discussion. A simple approach to the problem begins with the equation for a damped non-driven oscillator,

$$\ddot{x} + \gamma \dot{x} + \omega_o^2 x = o \qquad (10)$$

$$x = \rho - \rho_{min}(S) \qquad (11)$$

$$\Gamma = \frac{\gamma}{\sqrt{\omega_o^2 - \frac{1}{4}\gamma^2}} \qquad (12)$$

where γ is the damping coefficient (assumed constant) and w_o is the undamped harmonic oscillator frequency. The dimensionless damping coefficient is introduced in equation (12) and will be deduced from experimental measurements of the monopole oscillation characteristics. The variable ρ_{min} is the value of the density for which the excitation energy is a minimum for a given value of the entropy. The damping constant determines the rate at which energy is transferred to thermal energy from the collective motion thus determining the temperature. For a given value of the density, the entropy can be calculated thus fixing the value of ρ_{min}. The Skyrme interaction does not produce a true harmonic oscillation in the density coordinate but for reasonable excursions from the equilibrium density we shall use this approximation. A solution to such an equation is of the form

$$x \sim Ae^{-\gamma t/2}\cos(\omega t) \qquad (13)$$

where

$$\omega^2 = \omega_o^2 - \frac{1}{4}\gamma^2 \qquad (14)$$

The time required for disassembly is then

$$t = \frac{\pi}{\sqrt{\omega_o^2 - \frac{1}{4}\gamma^2}} \qquad (15)$$

The empirical full width at half maximum (FWHM) of the monopole excitation is typically ~4 MeV for an excitation energy of 15 MeV[6]. Table 2 illustrates how values of the damping constant influence the break-even temperature for the onset of the liquid-gas instability. In Fig. 1 the overstressed region is redefined assuming that the damping constant remains fixed at $\Gamma = 0.27$ (indicative of T=0 damping) and is not a function of temperature. One important point to note is that the minimum temperature required for the system to reach the unstable region can be determined from Fig. 1, noting the minimum excitation energy of the overstressed region which occurs at the intersection of the overstressed region boundary and the S/A=0 isentrope. Since energy is conserved, one can follow the line of constant energy to the boundary of the unstable region and then calculate the corresponding temperature from the corresponding density and energy. The resulting minimum observable temperature for a disassembly of this nature is 5.5 MeV. This is the minimum amount of energy transferred from the collective motion to the random thermal motion consistent with the damping deduced from the monopole oscillation width. This damping process also generates entropy. The minimum observable entropy can be calculated in a fashion similar to the minimum temperature and the final entropy at the unstable region boundary is 0.9. Hence a mechanical instability generates a minimum temperature of 5.5 MeV and minimum entropy of 0.9 prior to disassembly. The minimum excitation energy of the overstressed region is 4.75 MeV above the binding energy of normal nuclear matter (E = ~16 MeV) and $\rho \sim 1.5$ times normal nuclear density. The minimum incident energy required for an equal mass projectile and target system is 4 times the excitation energy, i.e. 19 MeV per nucleon. If 19 MeV per nucleon incident energy is insufficent to generate a system of 1.5 times normal nuclear density then the experimental minimum will be even larger. Initial entropies of greater than 2.0 appear to be affected much less than lower values of the initial entropy, hence this consideration does not contradict the cascade model calculations performed at higher energies which predict that entropy remains essentially constant during the expansion process[12].

The damping factor results in an enhancement of the time required for the system to reach the breakup region. The enhancement factor is

$$\Delta\tau = \tau - \tau(\Gamma = 0) = (\sqrt{1 + \frac{1}{4}\Gamma^2} - 1)\,\tau\,(\Gamma = 0) \quad (16)$$

resulting in an enhancement of 1-2%. Since Pauli blocking decreases with increasing temperature, the damping constant should also increase, further increasing the time available for chemical equilibration.

Conclusion

In summary, for temperatures greater than 8 MeV and less than the critical temperature a liquid-gas phase instability may manifest itself. If damping, as deduced from the monopole excitation, is taken into account, it appears that the oscillation time is increased by 1-2%. However, with increasing temperature, the damping constant becomes larger, and the available time for chemical equilibration will be greater. The damping also modifies the conditions for a mechanical instability particularly at low temperatures and low entropies. The redefinition of the overstressed boundary necessitates a corresponding increase in the incident energy of the projectile to permit the system to enter the unstable region illustrated in Fig. 1. For equal mass projectile and target, the minimum incident energy necessary is 19 MeV per nucleon in the lab frame which corresponds to an excitation energy of 4.75 MeV/u with a compression of 1.5 ρ_o, corresponding to S=0 and T=0, which will just place the system within the overstressed region defined for minimal damping, i.e. Γ=0.27. Subsequently, the system expands until it just reaches the unstable boundary where it has a temperature of 5.5 MeV and an entropy of 0.9, whereupon the system disassembles since the pressure will become positive. Consequently, observation of a mechanical instability, unperturbed by liquid-gas considerations, should be confined to temperatures greater than 5.5 MeV and less than -8 MeV.

1. M.W. Curtin, H. Toki and D.K. Scott, Phys. Lett. 123B (1983) 289.
2. H. Jaqaman, A. Mekjain and L. Zamick, Rutgers University Preprint RU-83-61 (1983).
3. P.J. Siemens, to be published.
4. G.F. Bertsch, Proc. Int. Conf. on Nucleus-Nucleus Collisions, ed. G.F. Bertsch, C.K. Gelbke and D.K. Scott, (East Lansing, 1982) to be published in Nucl. Phys.; G.F. Bertsch and P.J. Siemens, to be published.
5. L. Zamick, Phys. Lett. 45B, (1973) 313.
6. D.H. Youngblood et al, Phys. Rev. C23, (1981) 1997.
7. J. Cugnon, T. Mizutani and J. Vandermeulen, Nucl. Phys. A352 (1981) 505; H. Kruse, private communication.
8. J.S. Blakemore, in Solid State Physics (W.B. Saunders, Philadelphia, 1974) p.190.
9. D.K. Scott, in Dynamics of Heavy Ion Collisions, ed. N. Cindro, R.A. Ricci and W. Greiner (North-Holland, Amsterdam, 1981) p. 241.
10. S. Nagamiya et al., Phys. Rev. C24 (1981) 971.
11. H. Bohning, Proc. Int. Conf. on Nucl. React. Induced by Heavy Ions, 1970) p. 633.
12. G.F. Bertsch and J. Cugnon, Phys. Rev. C24 (1981) 2514.

TABLE 1

Nucleon evaporation times as a function of temperature assuming work functions of 8 MeV and 0 MeV.

T (MeV)	5	10	15	20
t ($\times 10^{-22}$ sec) W=8	6.9	0.77	0.27	0.13
t ($\times 10^{-22}$ sec) W=0	1.4	0.35	0.16	0.09

TABLE 2

The range of breadeven temperatures as deduced from the minimal and maximal work functions are given as a function of the number of sequential evaporation times required to achieve chemical equilibrium.

No. of Sequential evaporation time	Min $T_{b.e.}$ (W=0)	Max $T_{b.e.}$ (W=8)
1	5.0	8.1
3	8.7	12.1
10	15.8	19.4

TABLE 3

Breakeven temperatures for various values of the dimensionless damping constant and work function assuming emission of a single nucleon.

Γ / Γ (T = 0)	0	5	10	20
$T_{break\text{-}even}$ (MeV) W=8	8.1	7.6	6.9	5.8
$T_{break\text{-}even}$ (MeV) W=0	5.0	4.6	3.9	2.9